The effects of weak genetic perturbations on the transcriptome of the wing imaginal disc, and its association with wing shape in *Drosophila melanogaster*.

Authors: Ian Dworkin[1,2], Julie A Brown Anderson[1], Youssef Idaghdour[1] , Erin Kennerly Parker[1], Eric A. Stone[1] and Greg Gibson[1,3].

1- Department of Genetics, North Carolina State University.

2- Program in Ecology, Evolutionary Biology and Behavior, Department of Zoology, Michigan State University.

3- Center for Integrative Genomics, School of Biology, Georgia Institute of Technology, 310 Ferst Drive, Atlanta GA 30332.

Arrays submitted to GEO: GPL7740

Keywords: Genetic perturbations; complex traits;

Running Head: Expression profiling for subtle mutational perturbations

Keywords: wing shape, expression profiling, systems biology, quantitative genetics

Corresponding Author: Ian Dworkin

Department of Zoology,

203 Natural Sciences

Michigan State University

East Lansing, MI 48824

Email: idworkin@msu.edu

Abstract:

A major objective of genomics is to elucidate the mapping between genotypic and phenotypic space as a step toward understanding how small changes in gene function can lead to elaborate phenotypic changes. One approach that has been utilized is to look for the overall linear patterns of co-variation between phenotypic variables of interest, such as morphology, physiology and behavior, and underlying aspects of gene activity, in particular transcript abundance on a genome wide scale. Numerous studies have demonstrated that such patterns of co-variation do occur, although these are often between samples with large numbers of unknown genetic differences (different strains, or even species) or perturbations of large effect (sexual dimorphism, or strong loss of function mutations), that may represent physiological changes well outside of the normal experiences of the organism. In this study we utilized a mixed approach utilizing weak genetic perturbations of genes known to affect wing development in *Drosophila*, *melanogaster*, and contribute to differences in wing shape relative to a co-isogenic wild-type strain. We profiled the transcription of 1150 genes involved with or expressed during wing development in 27 heterozygous mutants, as well as their co-isogenic wild type and one additional wild-type strain. Despite finding clear evidence of expression differences between the mutants and wild-type, and across mutations, variation in gene expression did not appear to co-vary strongly with shape, suggesting that information from transcriptional profiling may not generally be predictive of final phenotype.

INTRODUCTION

Functional genomic research is dominated by two paradigms that derive their conceptual foundations from computer science and statistical genetics. Network biologists are interested in the patterns of connectivity between genes and gene products, and in the consequences that these patterns impose on properties of biological systems, such as metabolic flux or phenotypic robustness (Reeves, Muratov, Schupbach and Shvartsman 2006; Yakoby, Lembong, Schupbach and Shvartsman 2008; Yan, Zartman, Zhang, Scott, Shvartsman and Li 2009; Zartman, Kanodia, Cheung and Shvartsman 2009). Quantitative geneticists tend to be more linear in their search for association between genotypes and phenotypes (including gene expression), and their models generally assume a preponderance of additive effects of individual variants (Ayroles, Carbone, Stone, Jordan, Lyman, Magwire, Rollmann, Duncan, Lawrence, Anholt et al. 2009; Edwards, Ayroles, Stone, Carbone, Lyman and Mackay 2009; Passador-Gurgel, Hsieh, Hunt, Deighton and Gibson 2007). A major challenge for systems biologists is to unify these two frameworks through their studies of the genomic consequences of genetic perturbation.

An additional obstacle is that there are also two conceptually different approaches to perturbation analysis. One is to introduce large mutational or pharmacological changes to relatively homogeneous systems such as cell lines or clones of organisms in a highly controlled manner. While experimentally appealing, the perturbations are often well beyond the range of physiological or functional relevance, so the results may be difficult to generalize to actual biological circumstances. The alternative is to harness natural genetic or ecological variation, either in cross-sectional studies or in pedigrees and crosses (Ayroles, Carbone, Stone, Jordan, Lyman, Magwire, Rollmann, Duncan, Lawrence, Anholt et al. 2009; Edwards, Ayroles, Stone, Carbone, Lyman and Mackay 2009; Harbison, Carbone, Ayroles, Stone, Lyman and Mackay 2009; Passador-Gurgel, Hsieh, Hunt, Deighton and Gibson 2007; Rockman 2008). An advantage is that perturbation effects are averaged, and potentially replicated, over different genetic backgrounds, but the genomic effects of individual loci are generally subtle and only detected by statistical methods. They then require functional validation in more controlled experimental systems. Neither genome-wide association studies nor whole genome expression profiling have yet proven capable of consistently describing more than a fraction of the underlying genetic basis of phenotypic variation. Nevertheless, it is of interest to bridge these conceptual gaps by studying how local perturbations of gene function ramify throughout the complex of genetic pathways operating in cells, tissues and organisms. One common theme across paradigms is that transcriptional profiling studies, whether focused on large scale perturbations, or on comparisons across inbred lines derived from natural populations often lead to lists of differentially expressed genes that can number in the thousands. However, it can be difficult to

determine when changes in gene expression per se, facilitate trait expression. Thus it is clear that additional approaches must be sought out to ameliorate such observations.

Here we describe one complex model system for attempting such integration, namely the developing wing of the fruit fly *Drosophila melanogaster*. The wing imaginal disc is a well studied complex tissue from which the adult wing and parts of the thorax are derived (Held 2002). Genetic and environmental perturbations can result in both qualitative (Blair 2007; Garcia-Bellido and Santamaria 1972; Held 2002; Lawrence and Morata 1976; Waddington 1939) and quantitative morphological effects (Debat, Milton, Rutherford, Klingenberg and Hoffmann 2006; Dworkin and Gibson 2006; Mezey, Houle and Nuzhdin 2005; Palsson and Gibson 2000; Weber, Johnson, Champlin and Patty 2005). There is considerable segregating variation for adult wing size and shape in natural populations, and ecologically relevant variables such as temperature and nutrition contribute to the overall pattern of phenotypic variation observed for this species (Debat, Debelle and Dworkin 2009; Dworkin, Palsson and Gibson 2005; Palsson and Gibson 2004; Shingleton, Estep, Driscoll and Dworkin 2009; Zimmerman, Palsson and Gibson 2000). Wing shape in particular is an ideal "complex" trait. It represents a highly integrated multivariate phenotype (Dworkin and Gibson 2006; Klingenberg 2009; Klingenberg and Zaklan 2000), given that wing development requires the integration of numerous signaling pathways. These control not only the patterning of the wing blade (Brower 1986; Garcia-Bellido and Santamaria 1972; Lawrence and Morata 1976; Sanicola, Sekelsky, Elson and Gelbart 1995; Tabata and Kornberg 1994; Zecca, Basler and Struhl 1995), cell growth, proliferation and survival (Martin, Perez-Garijo, Moreno and Morata 2004), but also the specification, determination and maintenance of the wing veins whose placement provides the landmarks that are used to measure wing shape (Blair 2007).

In order to quantify the effect of weak genetic perturbation on the transcriptome, we have profiled gene expression in a panel of 27 heterozygous mutants (introgressed into a common genetic background) known to quantitatively perturb wing shape (Dworkin and Gibson 2006), in addition to the co-isogenic wild-type strain (Samarkand), and one additional wild-type strain (Oregon-R). A custom Illumina bead array was designed to interrogate the abundance of 1150 genes that are expressed in late third instar imaginal wing discs at the time of patterning of the future wing blade, when the wing margin, veins, and intervein regions are specified. The mutations, listed and annotated in Table 1, are due to P-element insertions in the genes, most of which have well-defined roles in mediating signals through the *Dpp* (TGF-β) and *Egfr* (receptor-tyrosine kinase) pathways. We have previously shown that wing phenotypes of the lines are significantly different from one another, but that they do not clearly correlate with the nature of the signal transduction pathway that is perturbed (Dworkin and Gibson 2006). The gene expression profiles are considered in relation to four possible hypotheses.

The null hypothesis, H_{0A}, is that despite showing morphological shape differences in the wing, the mutants do not demonstrate any evidence of differential expression. This unlikely null hypothesis needs to be considered carefully with respect to a more likely null, H_{0B}, which states that any expression differences between the mutant measured as a heterozygote and its co-isogenic wild-type will be too small to detect with the array platform. The phenotypic differences among lines typically involve slight displacements of the overall shape of the wing, or vein positioning, which are too subtle to see by eye and require careful quantitative, morphometric measurement to detect. Microarray technology resolves differences in expression as small as 1.2-fold with high confidence, so long as the effect is observed across the four or five replicates, but if the functionally important changes in expression occur in just a few percent of the cells of the developing imaginal disc at a precise time of development, or if expression differences are largely spatial, the experiment may be underpowered to detect differences.

The first alternate hypothesis, H_1, is that each mutant line is different from the others for some fraction of the transcriptome. The differences may involve different genes in different lines, or involve the same genes that are up- or down-regulated to varying degrees. Ideally, they would include changes in the expression of genes that are known targets of each specific mutation. Transcript abundance might also be correlated with aspects of the adult phenotype, leading to the identification of key mediators of phenotypic variation. Line-specific expression differences can be detected by analysis of variance of the ratio of the within-to-between line variance, noting that in this experiment, each microarray hybridization required scores of imaginal discs in order to obtain sufficient mRNA, so the within-line variance is mainly technical rather than biological.

The second alternate hypothesis, H_2, is that rather than each line being unique, there is a high correlation structure to the profiles of lines that share either a common biochemical perturbation, or give rise to similar adult wing shapes. For example, mutations that disrupt *Dpp* signaling ought to result in similar downstream effects on expression, and the differences between these lines may provide hints as to the ordering of gene effects, akin to classical epistasis analysis. Alternatively, lines with a relatively enlarged posterior compartment of the wing may differentially express a common suite of genes involved in posterior patterning. Such effects can be detected by cluster analysis of the average profiles of transcriptomes of each of the mutant lines, followed by supervised tests of correlation between expression and the genotypes or phenotypes.

Our analyses failed to lend strong support for either of these alternate hypotheses, and lead us to propose a third, H_3, that there is a significant correlation structure among lines, but that it suggests the existence of “attractor states” of gene expression (Huang, Eichler, Bar-Yam and Ingber 2005; Mar and

Quackenbush 2009). Almost twenty years ago, Stuart Kauffman in *The Origins of Order* (Kauffman 1993), proposed that the logical structure of gene networks will typically promote the channeling of development or physiology into alternate relatively stable states. The underlying logic of his mathematical models assumed Boolean on-off switches, and hence the attractor states could be visualized as matrices of on or off patterns of gene activity. Perhaps because gene expression is so clearly quantitative in nature, this idea has not been subject to empirical evaluation on the genome scale. Our data indicates that suites of hundreds of genes in perturbed wing discs adopt common expression profiles that do not clearly correlate either with the genetic perturbation or the adult phenotype, and lead us to reconsider the notion of stable genomic attractor states.

RESULTS

Validation of the Custom Gene Expression Platform

All of the effects described below involve subtle expression changes of hundreds of genes at levels that are at or below the threshold for detection by methods such as quantitative RT-PCR. Consequently, we have validated the custom Illumina bead array in two ways, namely by testing specific expectations, and by replicating a previously published experiment.

Of the 27 mutations used for this study, 17 were known to be located in putative non-coding regulatory regions of the genes of interest. Thus we expected that, measured across this subset of 17 mutants and their isogenic wild-type, the transcript abundance of the disrupted gene would be at a minimum in the line that carried the mutation. This was the case for 14 of the mutants, where the mutation reduces the expression of its own gene product (Figure 1, Table 1), providing good evidence that the microarray accurately quantifies the transcriptome. In the case of one gene (*dad*), one of two different probes was most highly expressed in the mutant line, implying up-regulation of gene expression, while the other was the least expressed. By and large these results are consistent with the demonstration that despite the use of very subtle perturbations of gene function, the Illumina focused array platform was sufficient to detect expression changes.

We recently published a detailed analysis of wing imaginal disc expression using the Bloomington Drosophila Genome Resource Center's whole genome oligonucleotide expression array to compare expression in *scalloped* mutants in two different genetic backgrounds (Dworkin, Kennerly, Tack, Hutchinson, Brown, Mahaffey and Gibson 2009). The core results of this experiment were replicated using the Illumina platform used in this study (data not shown). As many genes were found to

differ in expression between sd^{E3} mutants in the Sam and Oregon-R backgrounds as were found between mutant and wild-type discs, and the differential expression was enriched for distinct classes of gene, namely developmental patterning between strains and cell growth and division between mutant and wild-type. Results for specific transcripts were broadly comparable between the two platforms, with similar trends in relative abundance; however differences in statistical power, probe sequence, and labeling methods make it difficult to make more quantitative comparisons of the two platforms. Taken together, the good agreement between these two experiments, and the internal consistency of the Illumina array, validate the use of the bead array for quantification of imaginal disc gene expression.

Refutation of the null hypothesis of no differential expression

A first pass analysis of the effect of each mutation was performed by pair-wise comparison of the gene expression profiles of each strain against the Samarkand co-isogenic wild-type. As the strains were all generated by at least 15 generations of backcrossing, each differs from Samarkand only at a few percent of the genome surrounding the mutations. On average, only 1.4% (1.0% median) of the transcripts were seen to be differentially expressed ($p < 0.001$) in any of these pair-wise comparisons. Using a "q-value" FDR approach yielded similar results with evidence for 4.3% (0.9% median) of transcripts being differentially expressed. Thus, despite a clear indication that the effective reduction in gene expression can be detected for the transcripts of a given gene (given a mutation in that gene), individually, the weak effects of the perturbation have subtle influences on the transcriptome, much smaller than those seen for large scale perturbations or between wild strains.

Nevertheless, there is evidence for several potential novel interactions that are worth considering based on reciprocal patterns of mis-regulation. For example, in a *Gap1*/+ mutant heterozygote, there is evidence for an increase in expression of the *Dad* transcript relative to the Samarkand wild-type 2.53 (+- 0.17 SE) on a log2 scale (corresponding to 5.7 fold difference) . Reciprocally, in a *Dad*/+ mutant heterozygote there is a 1.1 (+-0.13 SE) increase in expression of Gap1 transcript, corresponding to a 2.14 fold difference,suggesting negative feedback between these genes. In addition, Hsp67Ba appears to be upregulated in 14 of the comparisons of heterozygous mutants to their samarkand wild-type, indicating the possibility of the activiation of a stress response. There were several other patterns of common alteration in expression that emerged when the effects on the transcriptional profile are examined on a gene by gene basis. Seven of the mutations (*Bs*, *sbb*/*mtv*, *babo*, *Mad*, *aos*, *ast*, *ksr*) show evidence for influencing the expression of CG30069. This gene has been shown to be upregulated in the wing imaginal disc (Butler, Jacobsen, Cain, Jarman, Hubank, Whittle, Phillips and Simcox 2003), and RNAi knockdown

of this gene induces a blistering phenotype, similar to the Bs gene (Jacobsen, Cain, Paul, Justiniano, Alli, Mullins, Wang, Butchar and Simcox 2006). In addition, 10 of the mutants (*Bs, Egfr, sbb, Gap1, Ptc, aos, babo, Mad, ast, ksr*), modulate the expression of X box binding protein-1 (Xbp1). Mutations of Xbp1 over a deficiency result in larvae without imaginal discs. Thus despite the small number (and small magnitude) of effects on gene expression, it is clear that these perturbations of small effect are sufficient to modulate expression of known regulatory genes in the developing wing imaginal disc.

Increased statistical power for detecting differential expression of genes among lines was gained by performing analysis of variance, contrasting the ratio of variance within lines (measured on between 4-6 arrays derived from paired discs manually dissected from 30 larvae each) to variance between. Figure 2a shows the relationship between significance of differential expression and the standard deviation between mutants. Evidence for differential expression can be observed across all levels of abundance. Adopting a sequential Bonferroni approach allowing for 1398 probes on the array, 270 probes were found to vary among mutants and their co-isogenic wild-type Samarkand. This number increased to 540 probes at the false discovery rate of $q<0.01$ (Storey and Tibshirani 2003), demonstrating differential expression among lines of at least one third of the genes on the microarray, and clearly refuting H_0. When the second wild-type (Oregon-R) is included in the analysis the number of probes deemed to be significantly different based on a sequential Bonferroni procedure is 324, or 528 at a q-value of <0.01. (Figure 2a) The genes are listed in Supplementary Table 1.

There is no obvious pattern of enrichment for probes corresponding to the 27 mutant genes in the list of most highly differentially expressed probes, suggesting that transcription in the two major signaling pathways downstream of the *Dpp* and the *Egfr* is not grossly disrupted in the lines. However, it should be noted that genes that are only differentially expressed in one or a few of the mutants will typically not be detected by ANOVA across the full panel. Thus, it is possible that substantial disruption of signaling in these pathways does occur in a small subset of the lines. Three of the genes did show a marginally significant tendency for differential expression in the *Egfr*-pathway mutant lines relative to the *Dpp* mutant lines (*ast* was downregulated; *babo* and *Mad* were upregulated), but the trend was weak in each case.

Weak evidence for co-variation between transcriptional variance and wing shape

The subtle genetic perturbations caused via the heterozygous effects of the mutations can be discerned using geometric morphometric techniques, as shown in Figure 3. Despite the fact that over 80%

of the mutations in the original study demonstrated a significant effect on shape (Dworkin and Gibson 2006), these effects are small relative to the differences between the two wild-type strains used in both the previous and current study. Indeed, Figure 3a demonstrates that the first canonical variate is largely due to the differences between the Samarkand and Oregon-R backgrounds, and not due to any individual mutations. By contrast, the second and third canonical variates separate *bs* and *ptc* mutant expression, as seen in Figure 3b).

Given these observations, we considered patterns of co-variation between gene expression and wing shape. Association of gene expression with wing shape was assessed using a subset of our previously reported wing shape data (Dworkin and Gibson 2006) corresponding to the mutations and genetic background used for gene expression profiling in the current study. First we utilized a multivariate regression approach, regressing shape onto gene relative gene expression for each probe. As shown in Figure 2b, while there is some evidence for associations between wing shape and expression, in general the degree of association is weak, as measured both using the p-value from probe specific models and the RV co-efficient, a multivariate version of the Pearson correlation co-efficient for co-variation between blocks of variables (Escoufier 1973). Indeed only the probe for the gene *Star* survived Bonferroni corrections for the multivariate regression, although two independent probes for *Bs*/*Dsrf* and a probe for *Delta* were among those with the highest RV co-efficients. We also utilized an alternative technique to assess patterns of co-variation between groups of genes and aspects of wing shape, 2 block partial least squares analysis (Klingenberg and Zaklan 2000; Rohlf and Corti 2000). This techniques utilizes the 2x2 matrix of covariances for gene expression data along with the phenotypic data and performs a singular value decomposition to extract the axes representing maximal co-variation between the 2 blocks (gene expression and shape: see methods). For statistical inference, 1000 permutations were performed to assess whether the observed patterns of co-variation between the blocks was extreme relative to the sampling distribution produced by permutation. When the full matrix of covariation for the shape variables was examined for association with the set of genes that were deemed to vary significantly across the weak genetic perturbations used in this study, only marginal evidence for an association was observed, none of which survived Bonferroni correction. This analysis refutes the strong version of $H_{1,}$ that each mutant produces a characteristic expression profile that co-varies with subtle aspects of the wing phenotype.

However, it is well known (Held 2002) that considerable temporal and spatial variation occurs for gene expression in the wing imaginal discs. Thus it was highly unlikely that we would observe an overall pattern of covariation between wing shape and the entire set of co-expressed genes. Consequently, we adopted a supervised exploratory approach in which we compared patterns of covariation between shape

and subsets of differentially expressed genes (as determined above) considered *a priori* based on their known functions. In Figure 4 we demonstrate the results from 2 block PLS for a number of candidate transcripts, or signaling pathways that have suggestive patterns of co-variation with shape. While none are formally significant after correcting for multiple comparisons, these represent candidates for future study. Given that 2 block PLS can be used for blocks of variables of arbitrary dimensions, we could theoretically scan all groups of transcripts in various block sizes and configurations for association with shape, however, it is unclear how any valid statistical inference could be made from such a large number of comparisons. Despite this, we examined a subset of genes that were differentially expressed that are all known to be involved with Dpp and Hh signaling, which help to specify the anterior-posterior patterning of the wing disc. As shown in Figure 4, the strongest associations with shape were observed for *bs* and *dad* transcripts, as well as for a composite measure of Dpp and Hh signaling, although these effects appear to be driven by a few datapoints. Interestingly genes involved explicitly with vein specification did not appear to associate with shape, nor did genes involved with insulin or TOR signaling (not shown).

We also examined the correlation between the number of genes deemed to be significantly expressed between mutants and their co-isogenic wild-type, and measures of distance between the mean shapes of the mutant and wild-type (Procrustes and Mahalanobis Distances). In both cases the correlations were at best, weakly suggestive (0.21 and 0.28 respectively), however the confidence intervals for both included zero.

Clustering of expression profiles identifies at least five networks of co-expressed genes.

Figure 5a (right side) shows Two-way hierarchical clustering was used to examine the overall co-expression structure, as illustrated by the heatmap in Figure 5a with probes represented by columns, and the 27 mutant lines as well as the two wild-type lines used in this study in rows. Each major grouping of mutant lines with similar profiles includes mutations in both the Dpp and EGF pathways. There is a hint of enrichment of the *Egfr* mutations in the top half of the plot, and *Dpp* in the bottom half, but permutation indicates that this partitioning is not significant. Notably, the dendograms generated via hierarchical clustering for the shape variables and for the transcripts deemed to be significantly different between lines, do not show a great deal of similarity (Figure 5a). This further confirms that there is no evidence for a high degree of co-variation between shape and transcript abundance measured in these heterozygous mutants. There may however be some smaller patterns linking small numbers of mutants since some similar profiles do fit prior expectations. Examples include the groupings of *Dpp*, *Dad*, and the two *tkv* introgressions, and of the two alleles of *mam* that are adjacent for both shape and gene

expression. On the other hand, there are also many couplings that do not separate out the pathways, such as *brk, S, sbb/mtv, & Bs*. The two alleles of *Mad* do not cluster together either for shape or gene expression, but $Mad^{kg00581}$ clusters with *ast* for both expression and shape.

The strong correlation structure observed in Figures 5a & b involves five or six groupings of mutants that cluster largely according to the expression of at least 5 sets of hundreds of genes. These mutant clusters are {*argos, asteroid, ksr,* $Mad^{kg00581}$*, babo, Egfr, drk, and Ptc*}, {*brk,S,sbb/mtv, Bs, Gap1*}, {*cbl, pnt,* SAM, (wild-type), *ed,* and the two *mam* alleles} , {*Dad, Dpp, spi* and both *tkv* alleles} & {*rho, rho-6,* Mad^{k00237}}. The alternative wild-type, Oregon-R, as expected appeared at the fursthest distance from all of the mutations which shared a common genetic background with Samarkand. Based on the these groupings, we identified five profiles as outlined in Table 2, and tested for the number of transcripts that significantly differentiate lines in each of these profiles.

A more formal modularity analysis was conducted using the Modulated Modularity Clustering (MMC) algorithm (Stone and Ayroles 2009) to simultaneously optimize the number of modules and linkages within them. From the 486 transcripts that showed evidence of differential expression, MMC identified 25 modules ranging in size from 2 to 75 genes (Figure 5c), with intra-module correlations ranging from 0.94-0.24 (mean of 0.75), which is higher than has been previously observed (Kocher 2010; Ayroles 2009}. This is likely due to the fact that the set of genes on the array represent a focused set of genes involved with similar biological processes. As demonstrated in the upper diagonal of Figure 5c, the amount of co-variation between modules is low, despite high correlation between individual transcripts within the modules. While specific gene ontology classes such as anterior-posterior lineage restriction or cuticle constituents were observed for most modules, in most cases these involved fewer than 10 genes and in no cases was significant enrichment observed after adjusting for multiple comparisons. We also utilized the MMC based clusters to re-examine the relationship between such modules and variation for shape. Focusing on the first 10 clusters, we performed two-block PLS, as described above. In no situation, were the singular values or the correlations across blocks, significant after correcting for genome wide comparisons. However. However, this is unlikely to reflect the overall biology as much as the fact that the focused array used for this was already highly enriched for genes that likely influenced wing development, and thus the whole set of probes are “pre-enriched”. Indeed Figure 5B demonstrates the very high degree of co-variation between transcript abundance across hundreds of genes among the set of genes that are differentially expressed.

DISCUSSION

The motivation for this study was to combine controlled perturbation analysis with gene expression profiling to characterize the genetic networks that may underlie quantitative differences in wing shape. We hypothesized that expression of a subset of genes active in the wing imaginal disc during a crucial patterning phase of wing development would either be associated with adult wing shape differences (H_1) and/or reflect the perturbation of the specific developmental pathway to which each mutation belongs (H_2). Despite overwhelming evidence for differential expression – one third of the genes showing differences among lines, and three quarters differences between supervised groups of lines, both of these hypotheses are rejected and it appears instead that the co-regulation of gene expression follows a different structure than that observed for the morphological effects for the mutations. Here we discuss the possible reasons for rejection of the alternate hypotheses and the implications of the possible existence of attractor states of expression.

Reasons for lack of association between gene expression and wing phenotype or mutant pathway

In retrospect it is perhaps not surprising that gene expression in mid-third instar imaginal discs is not clearly correlated with subtle aspects of adult wing shape. Noting that wing shape is largely invariant to size differences between the sexes and growth temperatures (after accounting for allometry), we have previously proposed that the placement and growth of the wing veins is a major determinant of wing shape, and that these act as a scaffold or mould for morphogenesis (Birdsall, Zimmerman, Teeter and Gibson 2000; Palsson and Gibson 2000). This would suggest that gene expression in the relatively small subset of the primordium that constitutes the vein fields is what is important, but quantitative changes in such cells may not be detectable by whole imaginal disc microarrays. By analogy, an aerial photograph of the foundations of a building under construction should indicate whether the structure will be square or rectangular, low-rise or high-rise, but probably will not indicate whether a skyscraper is 40 or 45 stories tall or whether the same floor plan carries through each story. Detailed expression profiling throughout the course of development may be necessary to detect associations with wing shape.

The rejection of the second alternate hypothesis, that expression differences would be most similar among lines that perturb the same developmental pathway, likely also relates to the complexity of the biology of the developing wing. It is known for example that the roles of genes in the *Egfr* pathway in specifying vein and intervein cellular identity switch in a matter of hours and over small sections of the disc (reviewed in (Held 2002)). Subtle expression differences in one set of cells are likely to be obscured by events occurring across the primordium: the wing disc is not like a population of uniform yeast cells or a mature tissue at equilibrium. Furthermore, patterning of the epithelium depends on interactions between

multiple signaling pathways including those mediated by the EGF, TGF, HH, and WNT growth factors, with extensive feedback and cross-talk. The network of gene expression across the imaginal disc is thus likely to reflect the impact of each mutational perturbation on each of these pathways, and may be more a function of the magnitude, location, and timing of the disruption than the pathway itself. Similarly, the analysis of co-variation across perturbations on wing shape did not suggest that perturbations in signaling pathways tended to have similar effects on shape (Dworkin and Gibson 2006).

Variation for gene expression: When does it impact the "phenotype"?

One fundamental assumption of many functional genomics studies is that there will be a direct relationship between transcriptional variation and the "ultimate" phenotype that is the target of the study (Ayroles, Carbone, Stone, Jordan, Lyman, Magwire, Rollmann, Duncan, Lawrence, Anholt et al. 2009; Passador-Gurgel, Hsieh, Hunt, Deighton and Gibson 2007). More specifically, it can be stated that there is an expectation that modulation of gene expression will contribute to phenotypic variation, in a predictable (if complex) manner. However, it is as yet unclear how much of the variation observed for gene expression or other intermediate phenotypes is phenotypically relevant, in that variation in the amount or activity of gene products results in a change in the trait value. In this study we demonstrated that while the expression of only a small subset of genes varied under any given perturbation, across the full set of perturbations several hundred genes showed evidence of differential expression. Yet variation in gene expression was found to only weakly co-vary with wing shape, despite the fact that the individual genetic perturbations substantially alter shape (Dworkin and Gibson 2006). This is contrary to other evidence which demonstrates much clearer patterns of co-variation between gene expression and behavioural, physiological or morphological phenotypes. Since in each of these cases it was a relatively small set of differentially expressed transcripts that was observed to co-vary with the target phenotype, it may be argued that much of the variation in gene expression is either noise, or is effectively filtered out before it can contribute to phenotypic variation.

In a recent study (Dworkin, Kennerly, Tack, Hutchinson, Brown, Mahaffey and Gibson 2009) we showed that despite a mutant in *scalloped* having a profound qualitative developmental defect in wing growth, the extent of gene expression variation (in terms of fold differences in expression) was much greater between two wild-type strains than between mutant and wild-type. This included a number of well known developmental regulators where 2-4 fold differences in expression would generally be expected to cause large developmental defects. This was not observed, and instead the mutant phenotype was associated with a set of differentially expressed genes that had relatively small effect sizes in comparison

to the differences between wild-type strains. It is clear that documenting differential expression of transcriptional co-variation is of itself insufficient to predict phenotypically relevant transcript abundance.

Indeed it is worth considering whether gene expression should ever really be considered in a univariate context, or whether it should be considered as part of a more diffuse multivariate structure. Instead of examining individual transcripts for associations with target phenotypes (Passador-Gurgel, Hsieh, Hunt, Deighton and Gibson 2007), we provide evidence that association between modules and target phenotypes should be evaluated (Stone and Ayroles 2009). Dpp pathways components, or wing margin determinants, collectively associate with aspects of wing shape, mirroring a recent report of association of modules of various classes of genes with behavioral attributes in adult flies (Ayroles, Carbone, Stone, Jordan, Lyman, Magwire, Rollmann, Duncan, Lawrence, Anholt et al. 2009; Harbison, Carbone, Ayroles, Stone, Lyman and Mackay 2009). The same objective, unsupervised MMC approach adopted by these authors did not reveal enrichment for gene ontology classes in our dataset and only weak association between shape and expression.

A possible contributing factor to the weak associations observed here, in addition to any noise of the measurements, is that the variation observed for this set of perturbations is quite small both for wing shape and gene expression. Given the design (genetic perturbations measured in an otherwise isogenic background in a controlled lab environment), our approach had a relatively high signal to noise ratio. Yet the perturbations used produced relatively little variation. The average effect size for shape differences between any given mutational perturbation and the wild-type was far smaller than that observed between two standard wild-type strains (Dworkin and Gibson 2006). We are currently testing this hypothesis by performing a similar experiment across a panel of inbred lines derived from natural populations that are segregating considerably more phenotypic variation for shape (Birdsall, Zimmerman, Teeter and Gibson 2000; Dworkin, Palsson and Gibson 2005; Palsson and Gibson 2004) and for gene expression (Ayroles, Carbone, Stone, Jordan, Lyman, Magwire, Rollmann, Duncan, Lawrence, Anholt et al. 2009; Passador-Gurgel, Hsieh, Hunt, Deighton and Gibson 2007).

Attractor states of gene expression in the developing wing primordium

At the gross survey level described here, there is a pervasive correlation to the dataset that requires explanation. The clustering of the transcriptome into four major sets of mutant lines with five major groups of hundreds of coregulated transcripts indicates a surprising degree of coordination of the activity of genes with diverse roles in cell growth and division, developmental patterning, morphogenesis,

and physiology. Hahn, Nuzhdin and colleagues (2008) described a similar phenomenon in a comparison of gene expression at two stages of embryogenesis in half a dozen lines of wildtype *D. melanogaster*, and performed a type of path analysis to infer that perturbation of gap or dorsal-ventral gene expression coordinates downstream changes. In our study, the perturbation is in all likelihood due to the mutations introgressed into a common genetic background, rather than to segregating polymorphism, but it is equally tempting to suggest that differential expression of five major regulatory genes leads to the downstream changes observed in the imaginal discs. These may be transcription factors characteristic of the groups of differentially expressed genes, though studies of yeast indicate that trans-acting expression modulators can have a variety of molecular functions.

Kauffman provided a framework for considering this coordination when he proposed that gene networks generally follow a Boolean logic that leads to stable attractor states. He predicted that stable networks absorb diverse perturbations or switch between alternate states, simply as a function of the structure of the networks (Figure 5). Thus, the minor perturbations due to heterozygous mildly deleterious transposable element insertions studied here, would be shaped by the pattern of response of cells across the imaginal disc, toward one of the relatively stable patterns of gene expression. It will be revealing to characterize the timing of establishment of these patterns as well as the extent to which they are maintained throughout development and in different environments.

The possible existence of attractor states of gene expression raises a number of interesting issues relating to the mapping of genotype onto phenotype. For network biologists considering how to dissect regulatory pathways from the correlation structure of expression profiles, it adds the challenge of predicting under what circumstances expression can be channeled into alternate networks. The models of von Dassow (von Dassow, Meir, Munro and Odell 2000) and colleagues are likely to be relevant in this regard as they have already shown that multiple different parameterizations of regulatory coefficients can support stable developmental patterning, for example in the establishment of the *Drosophila* wing margin (Yan, Zartman, Zhang, Scott, Shvartsman and Li 2009). For quantitative geneticists the results challenge the notion that additive genotypic effects on visible phenotypes arise via additive effects on gene expression. There is little evidence in our data for association between the clustering of mutant lines by transcription profiles, and their clustering by phenotype, implying that the gene expression states are not affecting the adult wing shape. This conundrum bares further investigation as it impinges on the buffering capacity of developmental systems, the relationship between differential gene expression and abnormality, including disease, and the capacity for neutral genetic drift in gene expression space.

Materials and methods

Fly lines, rearing and dissection: All of the mutants used are listed in Table 1. For each mutation the DNA lesion is caused by a P element transgenic insertion with a *w*+ rescue construct. As described previously (Dworkin and Gibson 2006) each mutation was introgressed via backcrossing into a common isogenic wild-type genetic background Samarkand (SAM) marked with a *w*- allele, a genetic background commonly used for quantitative genetic studies. Following introgression, each mutation was balanced against a balancer chromosome containing either p{w+, Ubi-GFP} or p{w+, act-GFP}. These balancer chromosomes were themselves repeatedly crossed into the SAM background (6-7 generations) prior to use so as to not introduce any additional segregating genetic variation.

For each line bearing the mutation (and corresponding balancer) males were crossed to virgin females of the w^-; SAM isogenic background. Larvae of each genotype were reared in low density conditions at 25 degrees C. At the wandering third instar stage, male larvae were rinsed in PBS, scored for the absence of GFP expression (indicating they were mutant/SAM). From these individuals, approximately 45-50 wing imaginal discs were dissected out and stored in RNAlater at -72C. For each line two replicate sets of dissections were performed on different days. The one exception is the isogenic wild-type w; SAM line where 6 independent dissections as outlined above were performed. In total ~ 4500 wing imaginal discs were used for the experiments described in this study.

RNA extraction, amplification and labeling: RNA extraction was performed using a modified protocol for the RNAeasy kit (Qiagen) as described previously (Dworkin et al. 2009). Following RNA extraction and purification, all samples were quality checked for 260/280 and 260/230 ratios using a NanoDrop spectrophotometer (Thermo Scientific, Wilmington DE).

We used the Illumina TotalPrep RNA amplification kit (Ambion Inc. Palo Alto CA) and followed the manufacturers protocol. Briefly, for each biological sample, two replicate sets of 500nG of total RNA was used in a reverse transcription reaction, followed by second strand synthesis of the cDNA. Following cDNA clean-up, an in-vitro transcription reaction was performed overnight with biotin labelled NTP's. Samples were then quantified and purity of the cRNA was confirmed.

Array design and Processing

Given that the primary goal of these experiments was to examine a candidate set of genes that influence wing development as opposed to gene discovery we designed a custom content array using the Illumina focused array platform (Illumina Inc. San Diego CA). This array contained genes known to affect wing development via direct loss of function phenotypes or their interacting partners. In addition we included

genes that appear to be expressed in the developing wing imaginal discs, and in particular show evidence of differential expression based on previous studies. (Butler, Jacobsen, Cain, Jarman, Hubank, Whittle, Phillips and Simcox 2003; Dworkin, Kennerly, Tack, Hutchinson, Brown, Mahaffey and Gibson 2009; Klebes, Biehs, Cifuentes and Kornberg 2002; Klebes, Sustar, Kechris, Li, Schubiger and Kornberg 2005; Li and White 2003). See Supplementary Table 1 for a list of genes included on this array, as well as probe sequences.

Given that the total number of samples hybridized (240) was far larger than the number of samples/array (16) we utilized an incomplete blocking strategy during hybridization so as to avoid confounding the effects of any mutation with array effects. Hybridization was performed following the manufacturers' protocol for the 16 sample Sentrix bead-array (Illumina Inc. San Diego CA). Briefly, 500nG of biotin labelled cRNA was mixed with hybridization buffer and formamide, and the sample was applied to the slide. Hybridization was performed overnight at 55°C with samples revolving in the chamber. Samples were then washed, blocked and incubated with strepavidin-Cy3 prior to a final washing and drying. The slide containing all 16 samples was scanned on an Illumina BeadStation. In total 240 samples were prepared and hybridized, including several samples that were re-hybridized when the first sample failed.

Despite the fact that each probe was represented by on average 30 independent beads randomly positioned on the array, large scale spatial artifacts or hybridization issues can always lead to potentially misleading results with solid state microrarrays. Therefore, each of the 240 array images were visually inspected for any large scale artifacts. In addition several samples failed to provide any signal, and were excluded from the analysis. MA plots of log transformed expression data were also examined for each array and were in general quite linear. Any arrays that demonstrated obvious signs of poor hybridization were excluded. Conservatively we used 216 of the arrays for analysis, of which 16 were for the replication of the study of Dworkin et al. 2009 [32]).

Analysis of the Illumina Sentrix array data

Given that the Illumina array platform is single channel, with 16 arrays/slide, data normalization is required to account for issues both with scanning (slide level variation) and any issues with labeling or hyrbidization (sample level issued). We examined both median and quantile normalized data, which both produced very similar results (not shown). As Median normalization provides a robust and simple approach, this was used for all analyses included here in the following probe (or gene) level models.

$$Gene_{ijklm} = \mu_i + G_{ij} + B_{ik} + GB_{i(jk)} + P_l + \varepsilon_{ijklm}$$

The model terms represent effects of the ith replicate of the jth genotype and the kth Batch, and P represents *l* different probes used to assess transcript abundance. For validation of the array performance by contrast with cDNA array data reported in [32], the Illumina expression data was somewhat smaller than the original experiment (4 samples per genotype/background), so we adopted a liberal q-value of 0.01 as our nominal cut-off for including genes deemed differentially expressed (Storey and Tibshirani 2003). Analyses were performed in both SAS (v9.1) and R V2.8 (R Development Core Team) using custom scripts (available on request).

Patterns of covariation between gene expression and shape

We utilized two different but related approaches to assess the degree of co-variation between wing shape and gene expression. First we utilized a multivariate linear model, regressing wing shape onto relative transcript abundance, fitting individual models for each probe. Given the statistical limitations of treating gene expression as predictor variables when only a small proportion of the total variation is accounted for, we also utilized 2 block partial least squares (Klingenberg and Zaklan 2000; Rohlf and Corti 2000). 2 block partial least squares, performs a singular value decomposition on the matrix of covariances between gene expression and shape variables (but without including variances and covariances from within the sets of either gene expression data, or shape data). Mathematically, we can represent this as follows:

$$\begin{vmatrix} \mathbf{S}_{11} & \mathbf{S}_{12} \\ \mathbf{S}_{21} & \mathbf{S}_{22} \end{vmatrix}$$

where $\mathbf{S}_{11}$ & $\mathbf{S}_{22}$ represent the variance co-variance matrices for shape variables, and gene expression variables respectively. $\mathbf{S}_{12}$ (with $\mathbf{S}_{21}$ being its transpose) represents the co-variation of variables between shape and gene expression, which is decomposed using singular value to extract eigenvalues and eigenvectors which represent a set of new variables, with the largest eigenvalue corresponding to the greatest degree of co-variation between variables (with eigenvectors representing the loadings on the original variables). Subsequent singular values obtained are uncorrelated (orthogonal) to all others. Analysis and visual shape descriptors from 2 block PLS were generated using morphoJ (Klingenberg 2008) with 1000 permutated data sets used to generate an appropriate sampling distribution to compare against the observed patterns of covariation. Results for the 2 Block PLS were verified using custom

scripts in R (Claude 2008). As a simple, scalar measure of degree of co-variation between shape and gene expression variables we utilized the RV co-efficient (Escoufier 1973; Robert and Escoufier 1976).

$$RV = \frac{\text{trace}(\mathbf{S}_{12}\mathbf{S}_{21})}{\sqrt{\text{trace}(\mathbf{S}_{11}\mathbf{S}_{11})\text{trace}(\mathbf{S}_{22}\mathbf{S}_{22})}}$$

Where the numerator can be interpreted as the total amount of co-variation between the shape and gene expression (Rohlf and Corti 2000). This differs from the first singular value from the 2-Block PLS which represents the maximum amount of co-variation between the 2 original sets of variables as described by a single vector for each set of original variables. The denominator can in turn, be interpreted as the total amount of variation in the two sets of variables, thus scaling the numerator (Klingenberg 2009), providing an expression analogous to the correlation co-efficient. RV was calculated using custom scripts in R V2.10.1 (Team 2009).

Modulated modularity clustering was used as previous described in (Ayroles, Carbone, Stone, Jordan, Lyman, Magwire, Rollmann, Duncan, Lawrence, Anholt et al. 2009; Stone and Ayroles 2009), with the transcript means (averaged across multiple probes) for the 486 transcripts with evidence for differential expression. This yielded a Q = 0.784, and k(number of estimated modules) of 25.

Acknowledgements: We would like to thank members of the Dworkin and Gibson lab for ongoing discussions about issues pertaining to this manuscript. Thanks to Julien Ayroles for discussions regarding analysis, and Shin-Han Shiu and Barry Williams for comments on the manuscript. The work in this manuscript was supported by grants MCB092234 and IOS09198555 from the NSF, and an NSERC PDF to ID and NIH 2R01 GM06100 to G.G.

References

Ayroles, J.F., M.A. Carbone, E.A. Stone, K.W. Jordan, R.F. Lyman, M.M. Magwire, S.M. Rollmann, L.H. Duncan, F. Lawrence, R.R. Anholt et al. 2009. Systems genetics of complex traits in Drosophila melanogaster. *Nat Genet* **41:** 299-307.

Birdsall, K., E. Zimmerman, K. Teeter, and G. Gibson. 2000. Genetic variation for the positioning of wing veins in *Drosophila melanogaster*. *Evolution and Development* **2:** 16-24.

Blair, S.S. 2007. Wing vein patterning in Drosophila and the analysis of intercellular signaling. *Annu Rev Cell Dev Biol* **23:** 293-319.

Brower, D.L. 1986. Engrailed gene expression in *Drosophila* imaginal discs. *Embo J* **5:** 2649-2656.

Butler, M.J., T.L. Jacobsen, D.M. Cain, M.G. Jarman, M. Hubank, J.R. Whittle, R. Phillips, and A. Simcox. 2003. Discovery of genes with highly restricted expression patterns in the Drosophila wing disc using DNA oligonucleotide microarrays. *Development* **130:** 659-670.

Claude, J. 2008. *Morphometrics with R*. Springer.

Debat, V., A. Debelle, and I. Dworkin. 2009. Plasticity, Canalization and Developmental Stability of the *Drosophila* Wing: Joint Effects of Mutations and of Developmental Temperature. *Evolution*.

Debat, V., C.C. Milton, S. Rutherford, C.P. Klingenberg, and A.A. Hoffmann. 2006. Hsp90 and the quantitative variation of wing shape in Drosophila melanogaster. *Evolution* **60:** 2529-2538.

Dworkin, I. and G. Gibson. 2006. Epidermal growth factor receptor and transforming growth factor-beta signaling contributes to variation for wing shape in *Drosophila melanogaster*. *Genetics* **173:** 1417-1431.

Dworkin, I., E. Kennerly, D. Tack, J. Hutchinson, J. Brown, J. Mahaffey, and G. Gibson. 2009. Genomic Consequences of Background Effects on *scalloped* Mutant Expressivity in the Wing of *Drosophila melanogaster*. *Genetics* **181**.

Dworkin, I., A. Palsson, and G. Gibson. 2005. Replication of an *Egfr*-wing shape association in a wild-caught cohort of *Drosophila melanogaster*. *Genetics* **169:** 2115-2125.

Edwards, A.C., J.F. Ayroles, E.A. Stone, M.A. Carbone, R.F. Lyman, and T.F. Mackay. 2009. A transcriptional network associated with natural variation in Drosophila aggressive behavior. *Genome Biol* **10:** R76.

Escoufier, Y. 1973. Treatment of Vector Variables. *Biometrics* **29:** 751-760.

Garcia-Bellido, A. and P. Santamaria. 1972. Developmental analysis of the wing disc in the mutant engrailed of Drosophila melanogaster. *Genetics* **72:** 87-104.

Harbison, S.T., M.A. Carbone, J.F. Ayroles, E.A. Stone, R.F. Lyman, and T.F. Mackay. 2009. Co-regulated transcriptional networks contribute to natural genetic variation in Drosophila sleep. *Nat Genet* **41:** 371-375.

Held, L.I.J. 2002. *Imaginal Discs : The Genetic and Cellular Logic of Pattern Formation*. Cambridge, Cambridge.

Huang, S., G. Eichler, Y. Bar-Yam, and D.E. Ingber. 2005. Cell fates as high-dimensional attractor states of a complex gene regulatory network. *Phys Rev Lett* **94:** 128701.

Jacobsen, T.L., D. Cain, L. Paul, S. Justiniano, A. Alli, J.S. Mullins, C.P. Wang, J.P. Butchar, and A. Simcox. 2006. Functional analysis of genes differentially expressed in the Drosophila wing disc: role of transcripts enriched in the wing region. *Genetics* **174:** 1973-1982.

Kauffman, S.A. 1993. *The Origins of Order: Self-Organization and Selection in Evolution*. Oxford.

Klebes, A., B. Biehs, F. Cifuentes, and T.B. Kornberg. 2002. Expression profiling of Drosophila imaginal discs. *Genome Biol* **3:** RESEARCH0038.

Klebes, A., A. Sustar, K. Kechris, H. Li, G. Schubiger, and T.B. Kornberg. 2005. Regulation of cellular plasticity in Drosophila imaginal disc cells by the Polycomb group, trithorax group and lama genes. *Development* **132:** 3753-3765.

Klingenberg, C.P. 2008. MorphoJ. Faculty of Life Sciences, University of Manchester.
Klingenberg, C.P. 2009. Morphometric integration and modularity in configurations of landmarks: tools for evaluating a priori hypotheses. *Evol Dev* **11:** 405-421.
Klingenberg, C.P. and S.D. Zaklan. 2000. Morphological intergration between development compartments in the Drosophila wing. *Evolution* **54:** 1273-1285.
Lawrence, P.A. and G. Morata. 1976. Compartments in the wing of Drosophila: a study of the engrailed gene. *Dev Biol* **50:** 321-337.
Li, T.R. and K.P. White. 2003. Tissue-specific gene expression and ecdysone-regulated genomic networks in Drosophila. *Dev Cell* **5:** 59-72.
Mar, J.C. and J. Quackenbush. 2009. Decomposition of gene expression state space trajectories. *PLoS Comput Biol* **5:** e1000626.
Martin, F.A., A. Perez-Garijo, E. Moreno, and G. Morata. 2004. The brinker gradient controls wing growth in Drosophila. *Development* **131:** 4921-4930.
Mezey, J.G., D. Houle, and S.V. Nuzhdin. 2005. Naturally segregating quantitative trait loci affecting wing shape of *Drosophila melanogaster*. *Genetics* **169:** 2101-2113.
Nuzhdin, S.V., D.M. Tufts, and M.W. Hahn. 2008. Abundant genetic variation in transcript level during early Drosophila development. *Evol Dev* **10:** 683-689.
Palsson, A. and G. Gibson. 2000. Quantitative developmental genetic analysis reveals that the ancestral dipteran wing vein prepattern is conserved in Drosophila melanogaster. *Development Genes and Evolution* **210:** 617-622.
Palsson, A. and G. Gibson. 2004. Association between nucleotide variation in *Egfr* and wing shape in *Drosophila melanogaster*. *Genetics* **167:** 1187-1198.
Passador-Gurgel, G., W.P. Hsieh, P. Hunt, N. Deighton, and G. Gibson. 2007. Quantitative trait transcripts for nicotine resistance in Drosophila melanogaster. *Nat Genet* **39:** 264-268.
Reeves, G.T., C.B. Muratov, T. Schupbach, and S.Y. Shvartsman. 2006. Quantitative models of developmental pattern formation. *Dev Cell* **11:** 289-300.
Robert, P. and Y. Escoufier. 1976. Unifying Tool for Linear Multivariate Statistical-Methods - Rv-Coefficient. *Journal of the Royal Statistical Society Series C-Applied Statistics* **25:** 257-265.
Rockman, M.V. 2008. Reverse engineering the genotype-phenotype map with natural genetic variation. *Nature* **456:** 738-744.
Rohlf, F.J. and M. Corti. 2000. Use of two-block partial least-squares to study covariation in shape. *Syst Biol* **49:** 740-753.
Sanicola, M., J. Sekelsky, S. Elson, and W.M. Gelbart. 1995. Drawing a stripe in Drosophila imaginal disks: negative regulation of decapentaplegic and patched expression by engrailed. *Genetics* **139:** 745-756.
Shingleton, A.W., C.M. Estep, M.V. Driscoll, and I. Dworkin. 2009. Many ways to be small: different environmental regulators of size generate distinct scaling relationships in *Drosophila melanogaster*. *Proc Biol Sci* **276:** 2625-2633.
Stone, E.A. and J.F. Ayroles. 2009. Modulated modularity clustering as an exploratory tool for functional genomic inference. *PLoS Genet* **5:** e1000479.
Storey, J.D. and R. Tibshirani. 2003. Statistical significance for genomewide studies. *Proceedings of the National Academy of Sciences of the United States of America* **100:** 9440-9445.
Tabata, T. and T.B. Kornberg. 1994. Hedgehog is a signaling protein with a key role in patterning Drosophila imaginal discs. *Cell* **76:** 89-102.
Team, R.D.C. 2009. R: A language and environment for statistical computing.
R Foundation for Statistical Computing.
von Dassow, G., E. Meir, E.M. Munro, and G.M. Odell. 2000. The segment polarity network is a robust developmental module. *Nature* **406:** 188-192.

Waddington, C.H. 1939. Preliminary Notes on the Development of the Wings in Normal and Mutant Strains of Drosophila. *Proc Natl Acad Sci U S A* **25:** 299-307.

Weber, K., N. Johnson, D. Champlin, and A. Patty. 2005. Many P-element insertions affect wing shape in *Drosophila melanogaster*. *Genetics* **169:** 1461-1475.

Yakoby, N., J. Lembong, T. Schupbach, and S.Y. Shvartsman. 2008. Drosophila eggshell is patterned by sequential action of feedforward and feedback loops. *Development* **135:** 343-351.

Yan, S.J., J.J. Zartman, M. Zhang, A. Scott, S.Y. Shvartsman, and W.X. Li. 2009. Bistability coordinates activation of the EGFR and DPP pathways in Drosophila vein differentiation. *Mol Syst Biol* **5:** 278.

Zartman, J.J., J.S. Kanodia, L.S. Cheung, and S.Y. Shvartsman. 2009. Feedback control of the EGFR signaling gradient: superposition of domain-splitting events in Drosophila oogenesis. *Development* **136:** 2903-2911.

Zecca, M., K. Basler, and G. Struhl. 1995. Sequential organizing activities of engrailed, hedgehog and decapentaplegic in the Drosophila wing. *Development* **121:** 2265-2278.

Zimmerman, E., A. Palsson, and G. Gibson. 2000. Quantitative trait loci affecting components of wing shape in Drosophila melanogaster. *Genetics* **155:** 671-683.

Figure legends

Figure 1: Illumina custom array based transcriptional profiling is sufficiently sensitive to observe small quantitative differences in expression due to weak mutational perturbations. Despite the small effects of the mutational perturbation (reducing transcription by < 50%), the arrays were able to clearly demonstrate reduction via the mutation. (a) and (b) Two independent probes of *Egfr* demonstrating reduced expression in the *Egfr* heterozygous mutant. Similarly for the *drk* probes for a *drk* mutation (c) and *spi* probes for a *spi* mutation (d).

Figure 2: Global transcriptional profiles and associations between wing shape and gene expression. (a) transcriptional profiles for 1398 probes representing ~ 1000 genes across all genotypes. Vertical axis is the transformed p-value for the overall linear model, while the horizontal axis represents the standard deviations between the genotypic means. Dashed horizontal line represents traditional Bonferroni correction for multiple comparisons. (b) Association of gene expression and variation for wing shape. The vertical axis is the transformed p-values from multi-variate regression of shape onto gene expression. The horizontal axis is the RV co-efficient, a measure of co-variation between gene expression and shape. The RV co-efficient is bounded between 0 (no co-variation) and 1 (complete co-variation).

Figure 3: Canonical variates (CVA) of the genotypes for wing shape variation. The left panel shows that CVA 1 represents the differences between the two wild type strains compared in this study (Oregon-R and Samarkand), while CVA 2 is largely due to the differences between the shape of the *Bs*/*DSRF* allele and all other genotypes. The right hand panel similarly demonstrates differences between the *Ptc* allele and the other genotypes. The illustrations represent the shape differences along the CV axis for the 9 landmarks with the remaining wing extrapolated using splines.

Figure 4: Associations between variation for wing shape and gene expression using 2 block partial least squares. To further describe the co-variation between wing shape and expression, we examined specific blocks of genes and shape. While few were significant, after correcting for the number of comparisons, several demonstrated interesting patterns worthy of description. Each panel represents the axes of maximal co-variation for shape and expression (a) *ventral veinless*, RV=0.17 (b) Dpp signaling components that demonstrated significant expression differences across genotypes (*bi*, *bs*, *dad*, *Gli*, *kni*, *Mad*), RV=0.33 (c) both probes of *bs*, with the largest RV co-efficient between shape and any transcript (RV=0.43); and (d) *dad*, RV=0.31. P-values (via permutation) are all $p \leq 0.05$.

Figure 5: Strong co-variation within gene expression, despite little similarity in clustering between expression and wing shape. (a) Topology for dendograms for shape (left) and expression (right) do not conform to one another.Multiple agglomeration rules and algorithms were utilized, which while varying in the exact topology, always demonstrated the lack of correspondence between shape and transcript abundance. Colors represent the clusters observed for the shape variables, and as can be observed those

clusters are not observed for the expression data. (b) clustering for gene expression based on correlations between transcripts demonstrates considerable amounts of co-variation in expression. (c) Modularity in gene expression profiles as determined by MMC [38] suggests covariation within and between estimated modules.The upper diagonal represents the estimated modules based on correlations of gene expression, with the colours representing cross-module correlations. The lower diagonals represents the overall pattern of correlation for individual transcripts (as in b, but arranged differently). Colors: red is correlation of 1, blue, -1 and green zero.

Table 1: List of mutations used in this study, and evidence that these mutations down-regulate their own expression. Evidence for reduced expression was based on the linear model presented in the methods section. P-value < 0.001 was considered strong evidence that the mutations caused the reduction in the expression of its own transcripts, while P-value < 0.01 was considered weak evidence.

gene symbol	allele	Transcript reduced in mutants?	location of TE insertion	Illumina Probe ID
aos	*W11*	**yes**	5' most exon near transcription start site	**2027**
ast	*KG07563*	**yes**	boundary of transcription start site and 5' UTR	**2208**
babo	*k16912*	**yes**	intron-exon boundary	**509, 910 (weak)**
brk	*KG08470*	no	5' of transcription start site	
Bs/DSRF	*k07909*	**yes**	unknown	**4271, 2932**
cbl	*KG03080*	**weak**	5' UTR	**4976**
Dad	*J1E4*	**yes**	intron	**3923**
Dpp	*KG08191*	no	3' of the gene	
drk	*k02401*	**yes**	unknown	**1182, 2166**
ed	*k01102*	**yes**	1st intron	**3366, 1309**
Egfr	*k05115*	**yes**	unknown	**2165, 1775**
Gap1	*mip-w[+]*	no	unknown	
ksr	*J5E2*	no	50kb upstream of ksr	
mad	*k00237*	no	CDS	
mad	*KG00581*	no	CDS	
mam	*BG02477*	no	intron	
mam	*KG02641*	no	intron	
pnt	*KG04968*	no	intron	
ptc	*k02507*	**yes**	intron	**4087**
rho-6	*KG05638*	*no transcripts on array*		
rho	*KG07115*	no	5' non-coding	
S	*k09530*	no	unknown	
sax	*KG07525*	no	5' UTR	
sbb/mtv	*BG01610*	no	intron or 5' UTR depending on transcript	
spi	*s3547*	**yes**	unknown	**5854, 3941**
tkv	*k16713*	**yes**	intron/5' non-coding-depends on transcript	**79, 5076 (weak)**
tkv	*KG01923*	**yes**	tkv intron, CG14033 transcript	**79, 5076 (weak)**

Supplementary Table 1: Illumina Probe IDs, Probe sequences, and results from global analysis across all mutant lines. The first two columns represent the name of the gene for the corresponding probe (ProbeID). Complete descriptions pertaining to this custom array can be found in accession GPL

7740. Columns 13-19 provide summary data pertaining to the global linear model across all mutants, not including the second wild-type strain, that differs from the genetic background of Samarkand (co-isogenic to all mutants). Num_DF: Numerator Degrees of freedom, Den_DF: Denominator degrees of Freedom, Pvalue: P value for the gene specific model; log10p: log transformed p values. Seq_Bon(log10): Sequential Bonferroni for the models based o number of comparisons. q-value: q-value (FDR) for the gene specific models. Columns 21-25 represent the same summary statistics for the gene specific models, but including the Oregon-R wild-type.

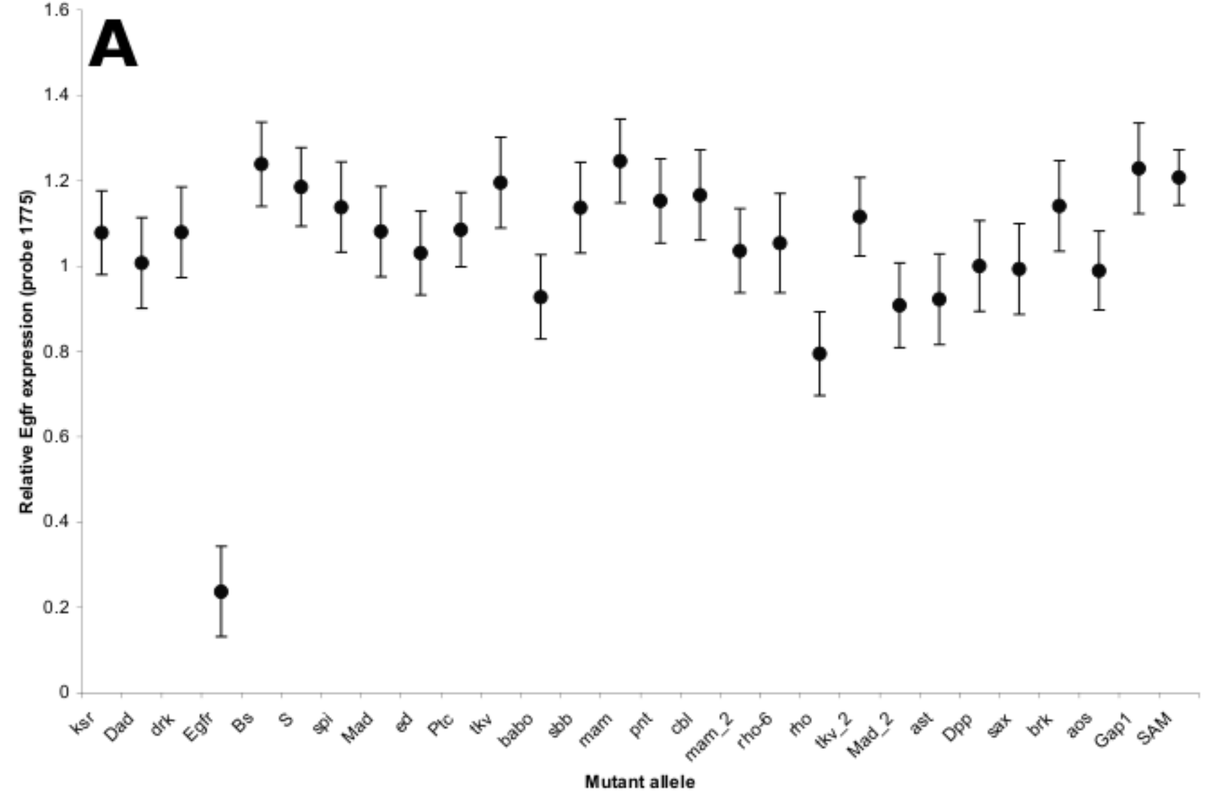
A
Relative Egfr expression (probe 1775)
1.6
1.4
1.2
1
0.8
0.6
0.4
0.2
0
ksr Dad drk Egfr Bs S spi Mad ed Ptc tkv babo sbb mam pnt cbl mam_2 rho-6 rho tkv_2 Mad_2 ast Dpp sax brk aos Gap1 SAM
Mutant allele

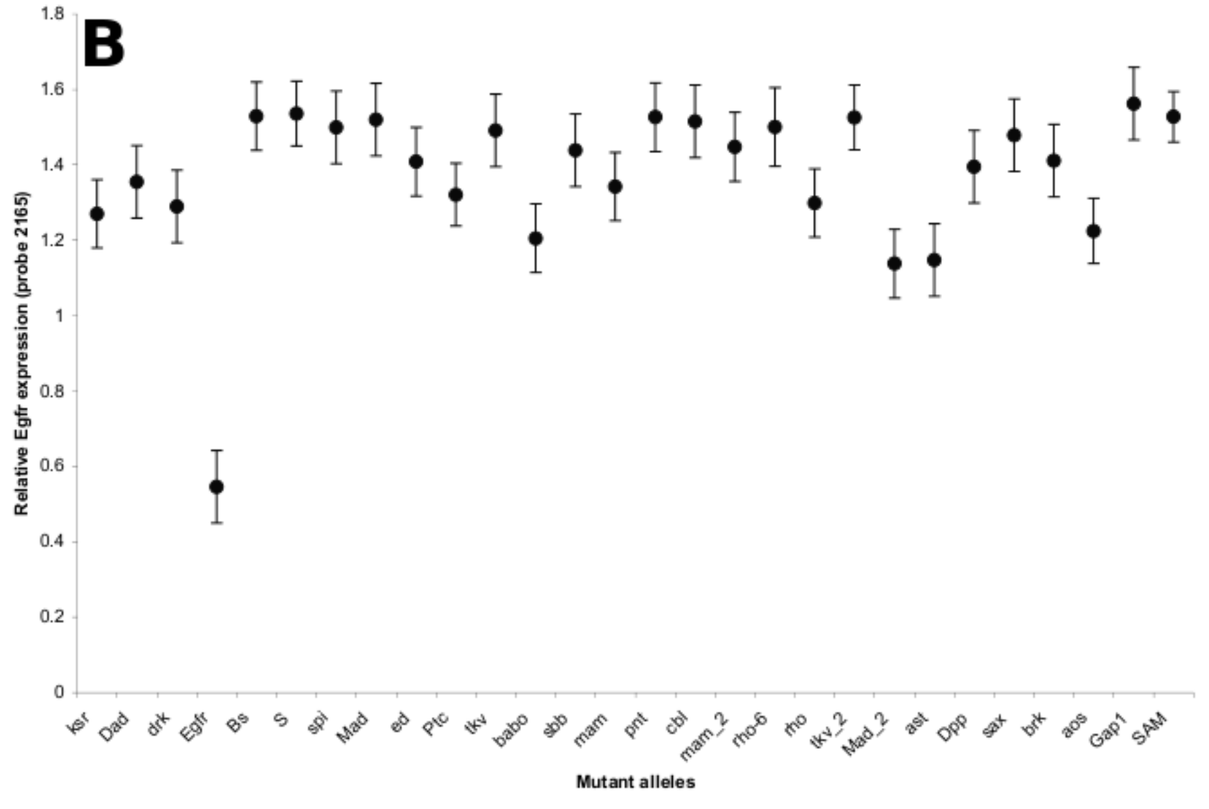
B
Relative Egfr expression (probe 2165)
1.8
1.6
1.4
1.2
1
0.8
0.6
0.4
0.2
0
ksr Dad drk Egfr Bs S spi Mad ed Ptc tkv babo sbb mam pnt cbl mam_2 rho-6 rho tkv_2 Mad_2 ast Dpp sax brk aos Gap1 SAM
Mutant alleles

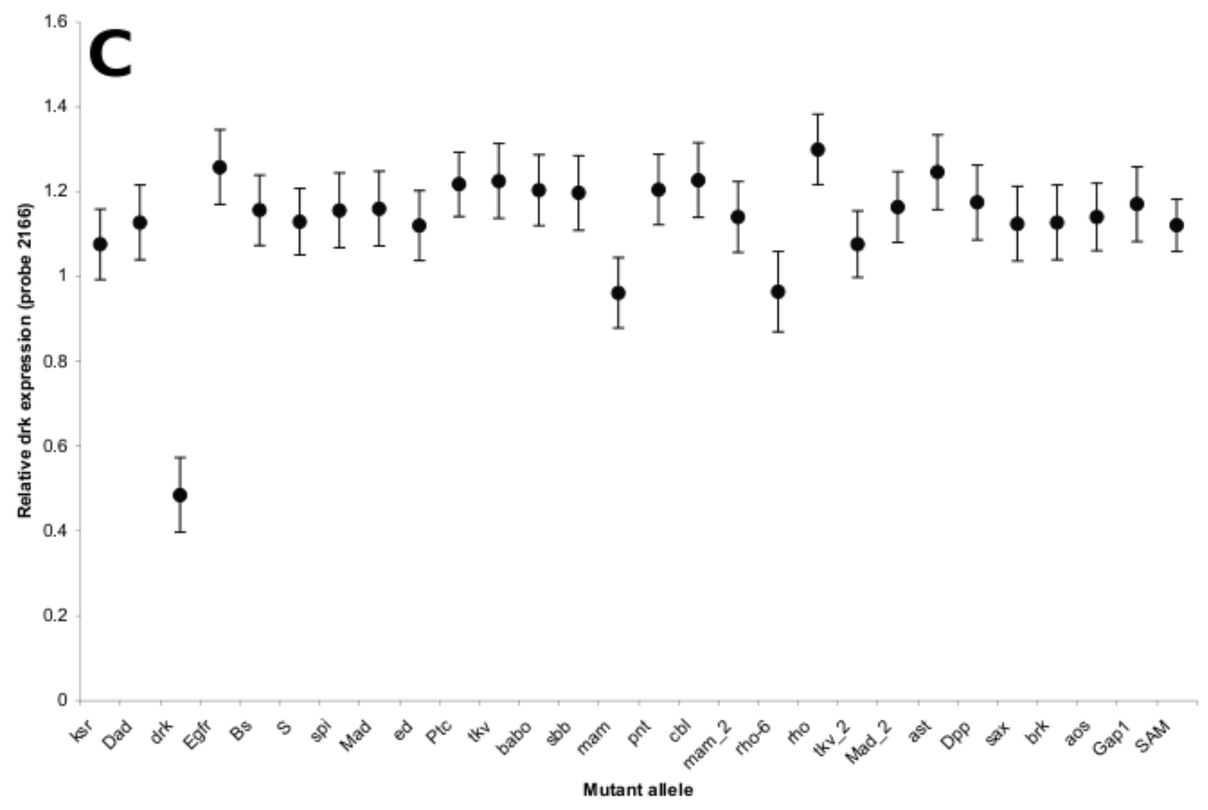
C
Relative drk expression (probe 2166)
1.6
1.4
1.2
1
0.8
0.6
0.4
0.2
0
ksr Dad drk Egfr Bs S spi Mad ed Ptc tkv babo sbb mam pnt cbl mam_2 rho-6 rho tkv_2 Mad_2 ast Dpp sax brk aos Gap1 SAM
Mutant allele

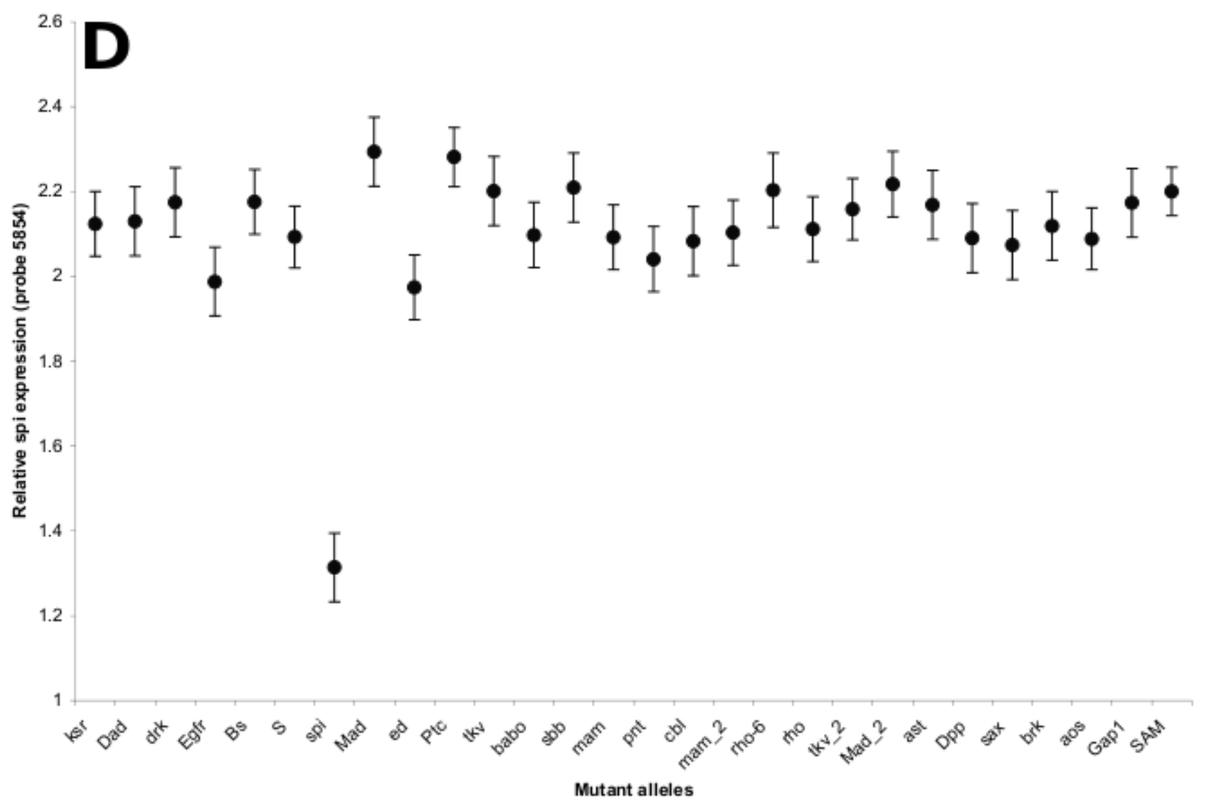
D
Relative spi expression (probe 5854)
2.6
2.4
2.2
2
1.8
1.6
1.4
1.2
1
ksr Dad drk Egfr Bs S spi Mad ed Ptc tkv babo sbb mam pnt cbl mam_2 rho-6 rho tkv_2 Mad_2 ast Dpp sax brk aos Gap1 SAM
Mutant alleles

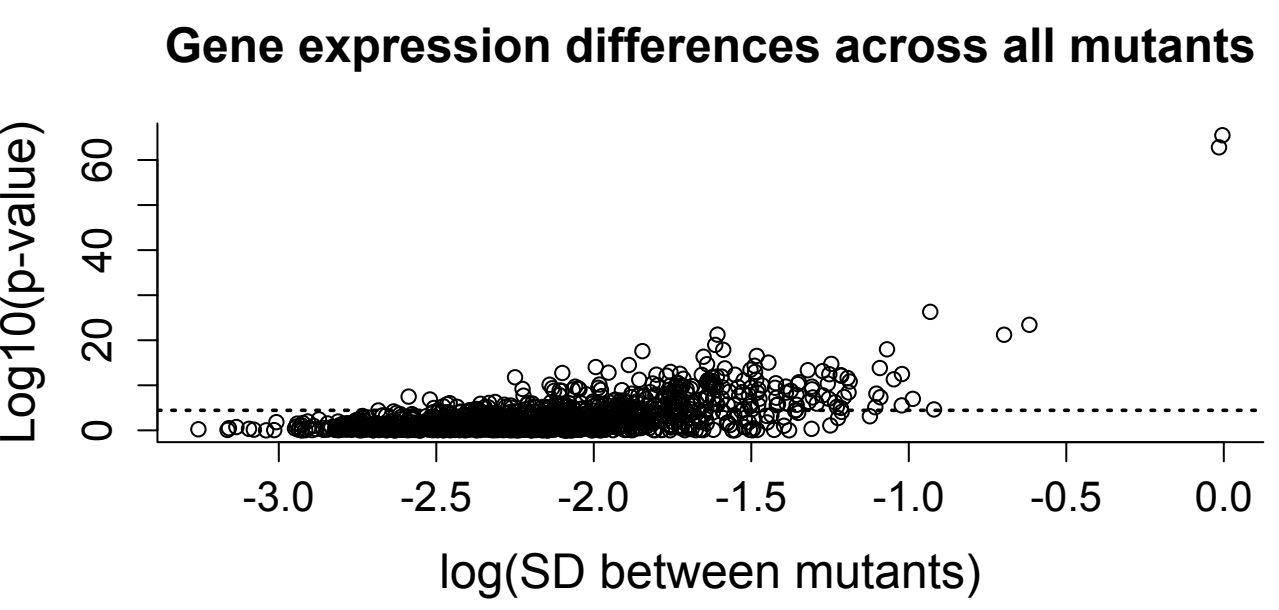
Gene expression differences across all mutants
Log10(p-value)
0
20
40
60
-3.0
-2.5
-2.0
-1.5
-1.0
-0.5
0.0
log(SD between mutants)

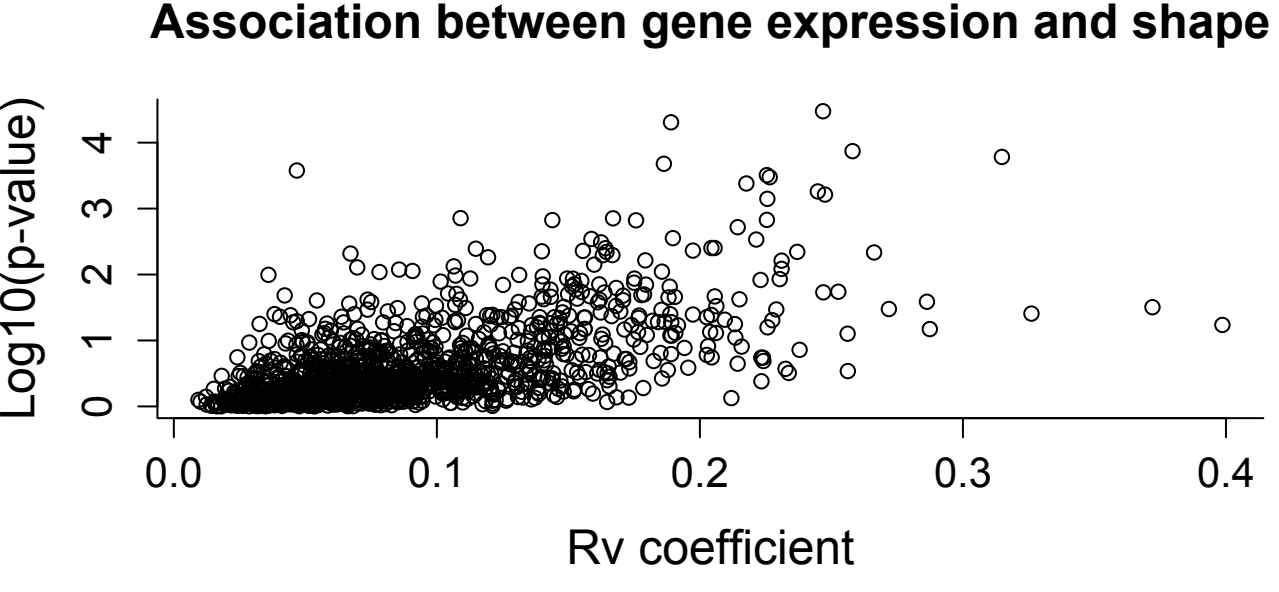
Association between gene expression and shape
Log10(p-value)
0
1
2
3
4
0.0
0.1
0.2
0.3
0.4
Rv coefficient

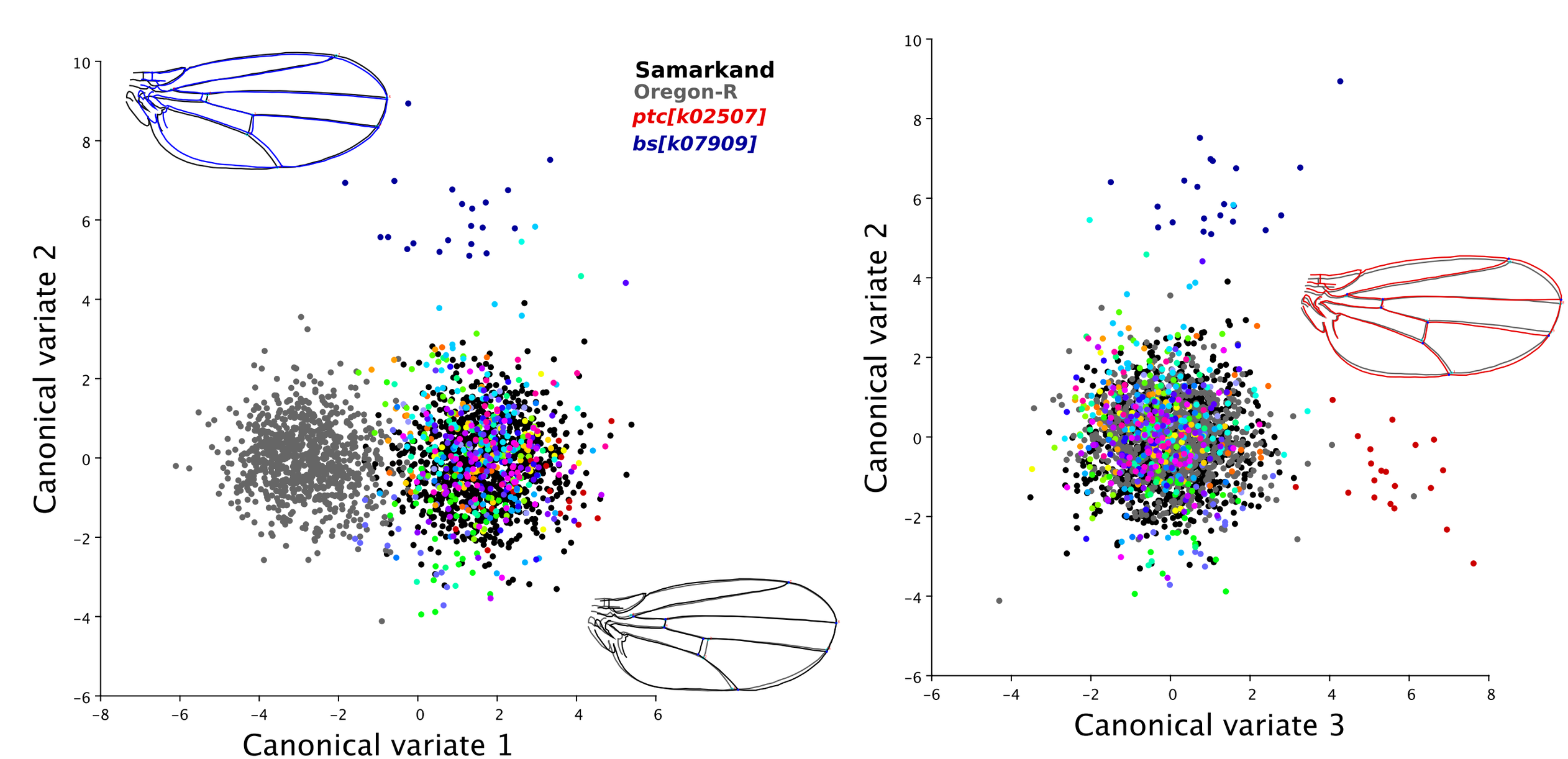
Samarkand
Oregon-R
ptc[k02507]
bs[k07909]
Canonical variate 2
Canonical variate 1
Canonical variate 2
Canonical variate 3

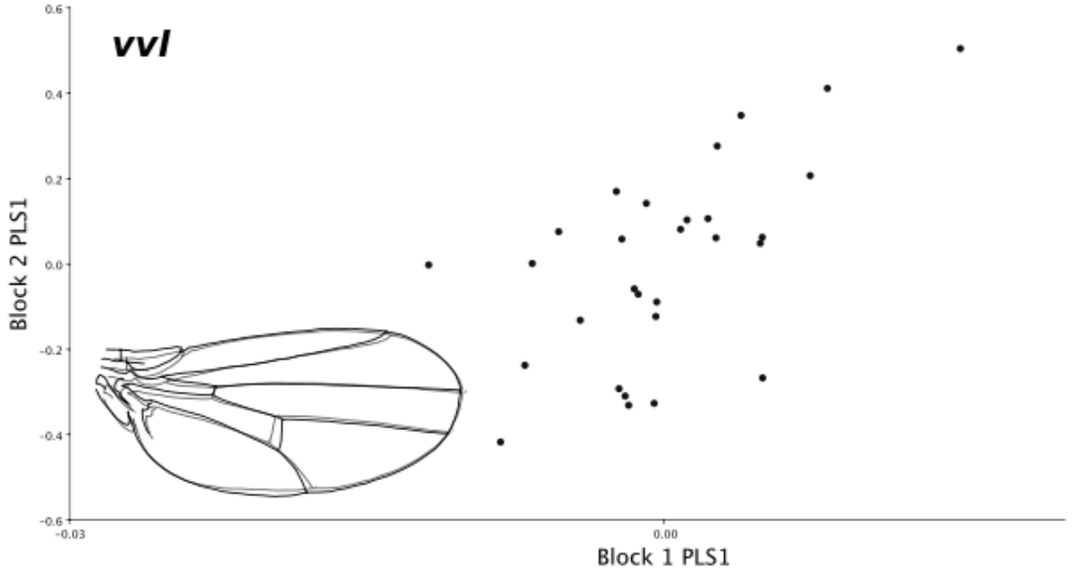
vvl
Block 2 PLS1
Block 1 PLS1
0.6
0.4
0.2
0.0
−0.2
−0.4
−0.6
−0.03
0.00

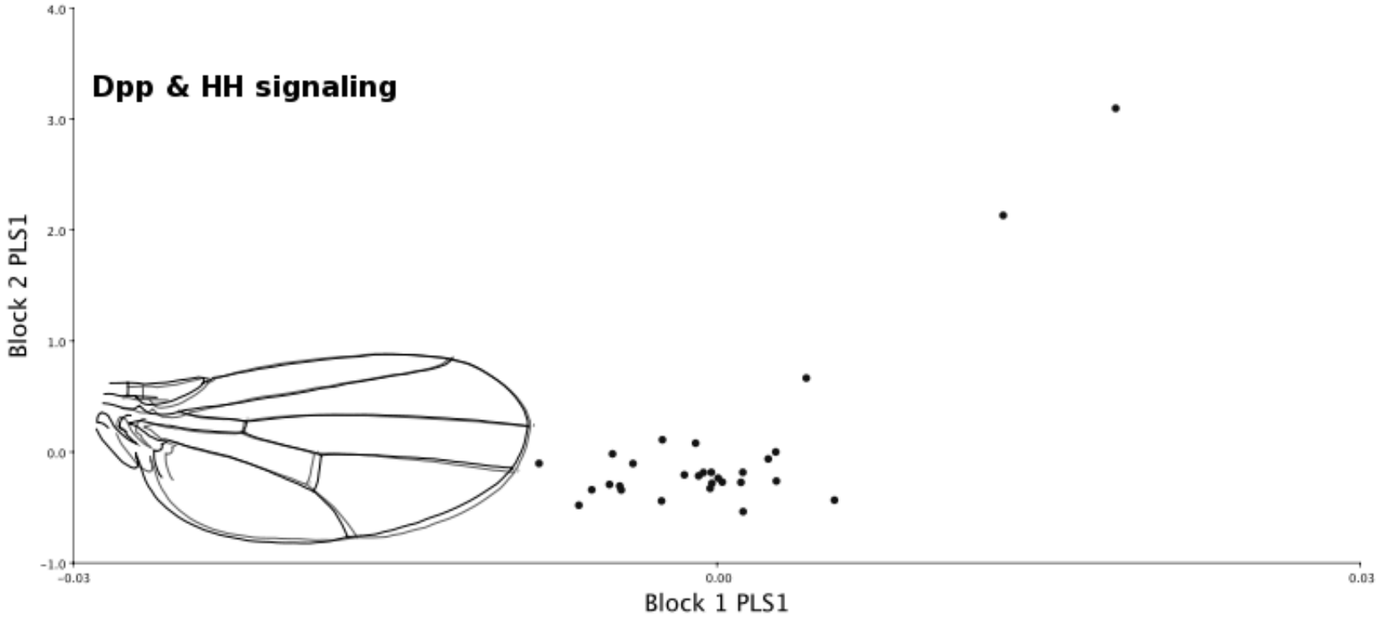
Dpp & HH signaling
Block 2 PLS1
Block 1 PLS1
4.0
3.0
2.0
1.0
0.0
−1.0
−0.03
0.00
0.03

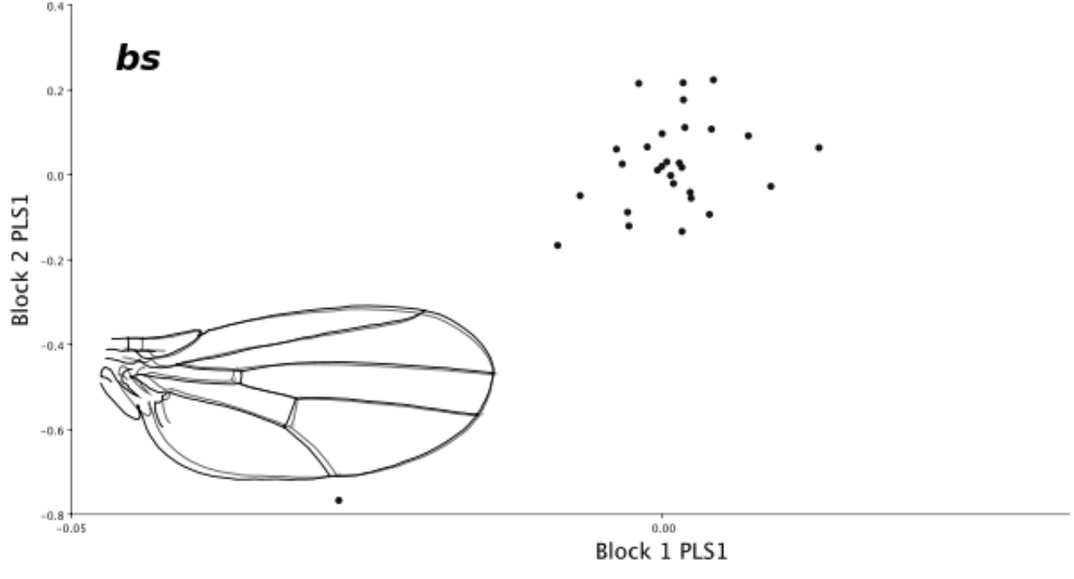
bs
Block 2 PLS1
Block 1 PLS1
0.4
0.2
0.0
−0.2
−0.4
−0.6
−0.8
−0.05
0.00

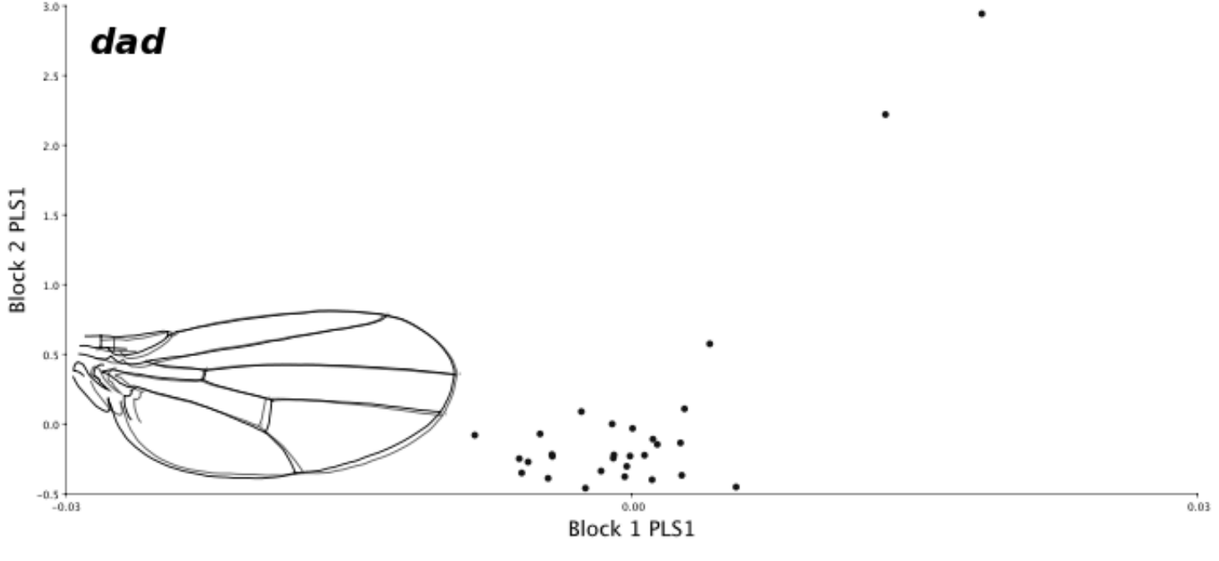
dad
Block 2 PLS1
Block 1 PLS1
3.0
2.5
2.0
1.5
1.0
0.5
0.0
−0.5
−0.03
0.00
0.03

A

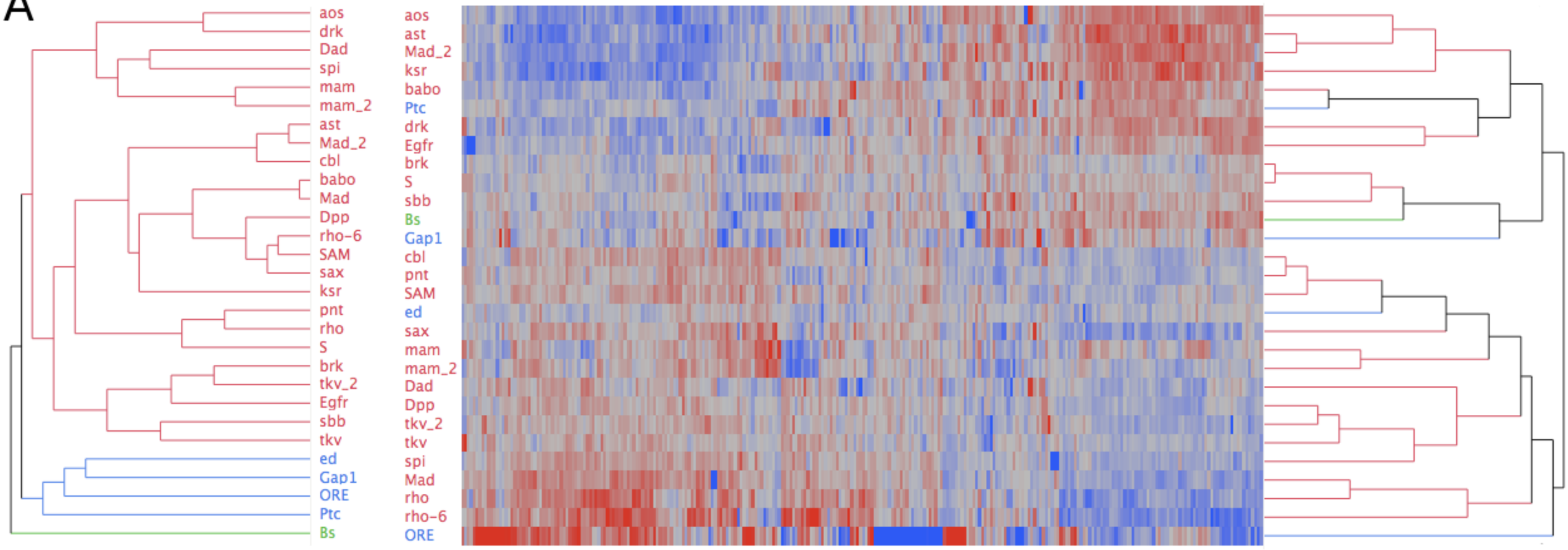
aos
drk
Dad
spi
mam
mam_2
ast
Mad_2
cbl
babo
Mad
Dpp
rho-6
SAM
sax
ksr
pnt
rho
S
brk
tkv_2
Egfr
sbb
tkv
ed
Gap1
ORE
Ptc
Bs
aos
ast
Mad_2
ksr
babo
Ptc
drk
Egfr
brk
S
sbb
Bs
Gap1
cbl
pnt
SAM
ed
sax
mam
mam_2
Dad
Dpp
tkv_2
tkv
spi
Mad
rho
rho-6
ORE

B

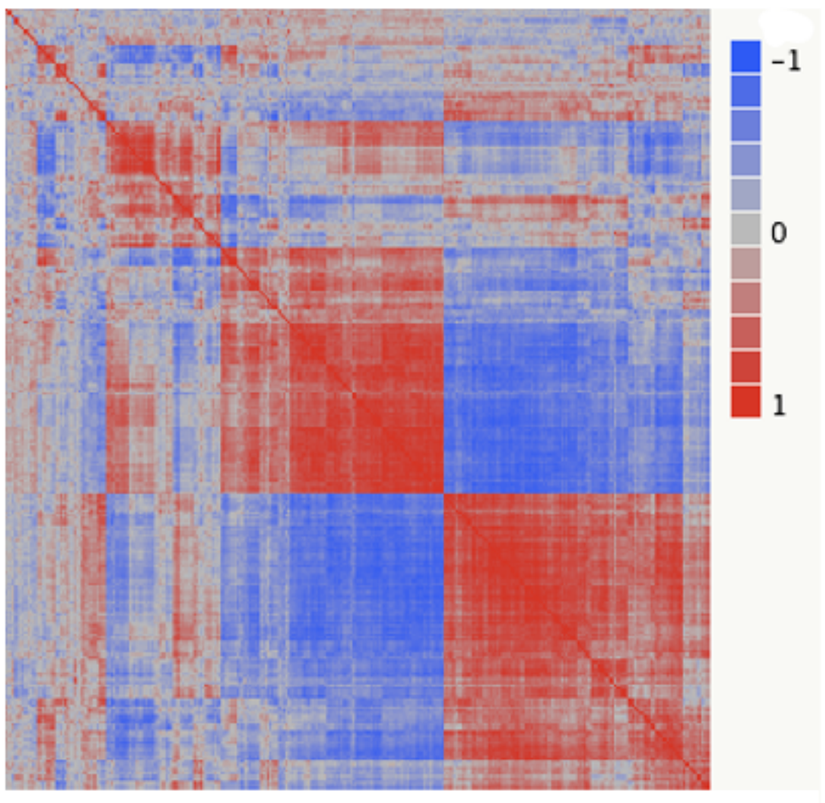
-1
0
1

C

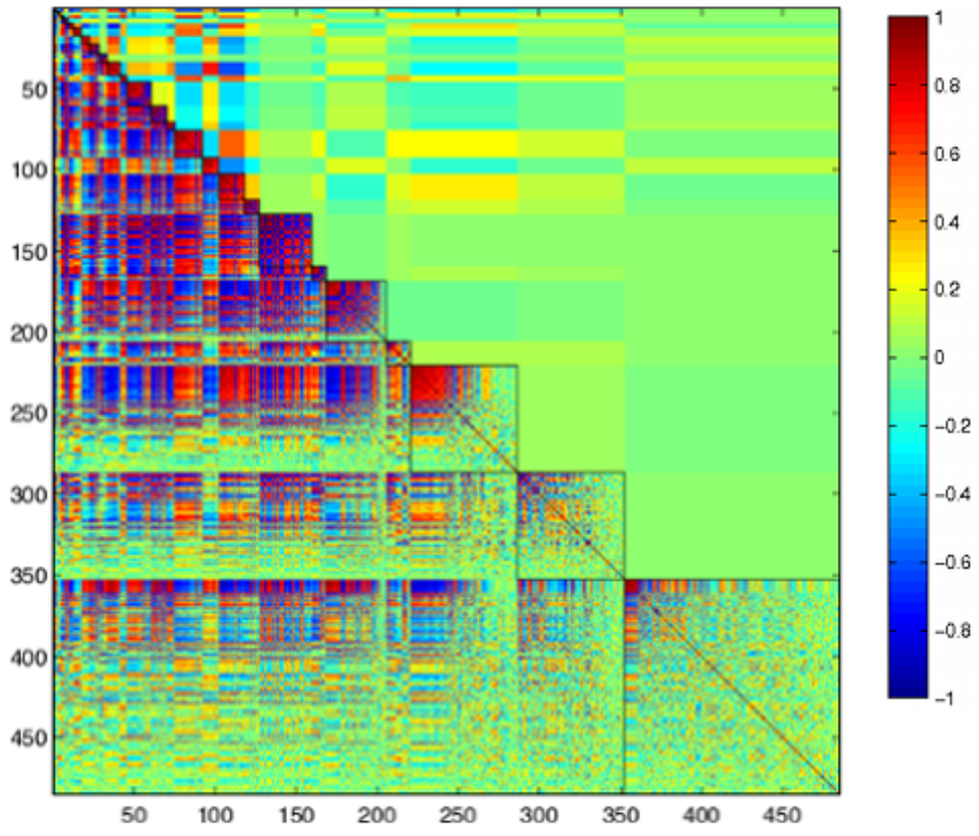
50
100
150
200
250
300
350
400
450
1
0.8
0.6
0.4
0.2
0
-0.2
-0.4
-0.6
-0.8
-1